Hydrodynamic Analysis of Shallow Water Sloshing in Ship Chamber Under Longitudinal Earthquake

Jianbao Yang[1], Yang Zhang[2,*] and Duanwei Shi[3]

[1]*School of Medicine and Health Sciences, Xianning Medical College, Hubei University of Science and Technology, Xianning 437100, P.R. China*
[2]*Institute of Engineering and Technology, Hubei University of Science and Technology, Xianning 437100, P.R. China*
[3]*Key Laboratory of Hydraulic Machinery Transients (Wuhan University), Ministry of Education, Wuhan 430072, P.R. China*
E-mail: yangjianbao@hbust.edu.cn; zhangyang619@hbust.edu.cn; 304492060@qq.com
[*]Corresponding Author

Abstract

Shallow water sloshing-structure interaction under the coupled longitudinal and pitch motions resulted by the longitudinal earthquake directly affects the structural safety of the shiplift. However, no matter in shiplift or other related fields, there is little research on this aspect at present. As a basis of structural dynamics analysis and earthquake resistant design, an analytical method including a developed modal system and new engineering formulas is presented to predict the hydrodynamic moment and force in the ship chamber. Based on the linear modal theory, a modal system describing shallow water sloshing under longitudinal earthquake is developed with infinite set of modal functions. Then, new engineering formulas for calculating the hydrodynamic

moment and force are proposed with only retaining the lowest sloshing mode ($n = 1$). Case simulations suggest that the maximum error of hydrodynamic moment and force between $n = 1$ and $n = 100$ are lower than 1.3% and 10.5%, respectively. In addition, the hydrodynamic moment resulting from pressure on the walls can be reasonably ignored, which accounts for less than 0.5% percent of total hydrodynamic moment. With respect to the currently used Housner model, the presented formulas are greatly improved in computational accuracy and rationally supplement the missing part in the seismic design part of the Design code for shiplift.

1 Introduction

It is well recognized that shallow water sloshing in the ship chamber would cause tremendous hydrodynamic moment and force, which will affect the safe operation of the shiplift. Therefore, the shallow water sloshing-structure interaction should necessarily be considered for the structural dynamics analysis and earthquake resistant design of the shiplift. Currently, almost all scholars who study the shiplift directly use the Housner model [1–3] to simulate the sloshing. Although simple, the computational accuracy is not ideal. In order to improve the accuracy of engineering calculation and ensure the safety of shiplift under extreme conditions, the shallow water sloshing-structure interaction in the shiplift system should be studied in depth. Especially a more accurate analytical method predicting the hydrodynamic moment and force is urgent to be developed.

Previous studies always simplify the ship chamber movements into a single motion [4, 5]. But in actual conditions, it might be simultaneously happened by longitudinal, vertical, and pitch motions [6]. Numerical results [7] show that there is nearly twofold increase in the peak magnitude, and the peak sloshing pressure is observed to be maximum when the coupled longitudinal and pitch motions are in phase. The coupled longitudinal and pitch motions should be further researched, especially the shallow water sloshing under the coupled motion, which are the key factors affecting the safety and reliability of the shiplift. The purpose of this paper is to develop the linear mode theory to simulate the shallow water sloshing in the ship chamber under the longitudinal earthquake.

General sloshing in rectangular tank has been studied based on the potential flow theory during the past decades [8–12]. But for the shallow water sloshing in the rectangular ship chamber, fewer researchers have provided analytical solutions. For instance, Liao [13] firstly introduce the Housner theory to research the sloshing in the ship chamber. Although not perfect, it provides a useful attempt. More than this, the Housner model is also applied to the transverse seismic design in the Design code for shiplift. Apart from the shiplift field, Li et al. [14, 15] give a supplementary, exact solution to the Housner model, and extend the implications to the aqueduct bridge. The Housner model has provided an easy way to calculate the hydrodynamic pressure under single motion. But for the ship chamber with coupled motions, it may not appropriate to directly use the Housner model.

The shallow water sloshing under the coupled motions should be highly concerned, which is seldom researched both in shiplift and other related fields. The study conducted by Verhagen and Wijngaarden [16] applies the one-dimensional gas flow theory to the fluid oscillations and calculates the shape of the hydraulic jump under pure sway or roll motion. The investigation carried out by Antuono [17–20] implements a modal description and formulas of the global force and moment for the most violent breaking cases. The above observations mainly focus on the nonlinear shallow water sloshing. But according to the running observation of the currently used shiplifts and the "Safety and Reliability Assessment Report of the Three Gorges Water Conservancy Shiplift (Comprehensive Report)", almost no nonlinear and no water resonance occur even under earthquake condition. Introducing a linear shallow water sloshing theory is enough for the shiplift design.

The linear modal theory, as described by Faltinsen and Timokha [21–24], Strand and Faltinsen [25], and Kolaei et al. [26], has shown reasonable accuracy when applied to compute the hydrodynamic loads with a few natural modes. The aim of the presented contribution is to develop the linear modal theory to simulate the shallow water sloshing under longitudinal earthquake. This being a missing aspect in the nearly all previous studies about seismic design of the shiplift.

In the presented study, to extend the use of the linear modal theory to the shiplift problems, a modal system will be developed to describe the shallow water sloshing in the ship chamber under coupled longitudinal and pitch motions. Hydrodynamic moment and force shall then be derived relying on the Euler equations and the separation of variables. New engineering formulas for calculating the hydrodynamic moment and force would be proposed

with only retaining the lowest sloshing mode, which aim to supplement the missing part of the longitudinal earthquake resistant design in the Design code for shiplift. It is conducive to improving the navigation safety of ships and the operation safety of shiplift.

2 Mathematical Formulations

2.1 Shallow Water Sloshing Under Coupled Motions

When the shiplift is encountered longitudinal earthquake, the excitation will be transmitted to the ship chamber through the tower column and guide device. Then the ship chamber will be subjected to coupled longitudinal $x(t)$ and pitch $\alpha(t)$ motions. The relative position relationship and the key position between the ship chamber, water and ship under longitudinal earthquake is displayed in Figure 1. H is the effective water depth, H_s is the immersion depth of ship, L is the ship chamber length, L_s is the ship length, $o'x'z'$ is the earth-fixed coordinate system, and oxz is the ship chamber-fixed coordinate system. The draft of a 3000t cargo ship accounts for about 75% (H_s/H) of the effective water depth, and the length accounts for about 73% (L_s/L) of the ship chamber length.

According to the design code for shiplift and reference [4, 5, 13, 27], the influence of ship can be reasonably simplified in the engineering hydrodynamic calculation. When the ship chamber is subjected to pure pitch motion, it rotates counterclockwise around the y-axis in the *xoz* plane. The absolute velocity potential $\Phi_P(x, z, t)$ can be expressed as the reference [27].

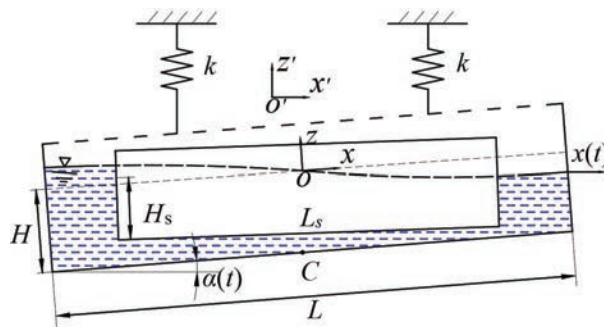$$\Phi_P(x, z, t) = \Phi_P^R(x, z, t) + \Phi_P^S(x, z, t) \tag{1}$$

Figure 1   Location of the ship chamber, ship and water under the coupled longitudinal $x(t)$ and pitch $\alpha(t)$ motions.

$$\Phi_P^R(x, z, t) = \dot{\alpha}(t)\varphi_{sj}(x, z) \tag{2a}$$

$$\varphi_{sj}(x, z) = -xz + \sum_{n=1}^{\infty} \frac{4L^2[(-1)^n - 1]}{\pi^3 n^3}$$

$$\times \cos\left[\pi n\left(x + \frac{L}{2}\right)\bigg/L\right] \frac{\sinh\left[\pi n\left(z + \frac{H}{2}\right)\big/L\right]}{\cosh\left(\frac{\pi n H}{2L}\right)} \tag{2b}$$

$$\Phi_P^S(x, z, t) = \sum_{n=1}^{\infty} \frac{\dot{\beta}_n^P(t)}{\kappa_n} \cos\left[\pi n\left(x + \frac{L}{2}\right)\bigg/L\right] \frac{\cosh\left[\frac{\pi n(z + H)}{L}\right]}{\cosh\frac{\pi n H}{L}} \tag{3}$$

here the velocity potential $\Phi_P^R(x, z, t)$ represents the rigid body motion of the fluid. The velocity potential $\Phi_P^S(x, z, t)$ represents the liquid motion relative to the container. $\varphi_{sj}(x, z)$ is the Stokes-Joukowski potential associated with the pitch motion of the ship chamber. $\kappa_n = \frac{\pi n}{L}\tanh(\frac{\pi n H}{L})$. $\beta_n^P(t)$ are the infinite set of generalized coordinates of the natural sloshing modes under pure pitch motion, which could be written as:

$$\ddot{\beta}_n^P(t) + \omega_n^2\beta_n^P(t) = \frac{4L}{\pi^2 n^2}\left[g\kappa_n\alpha(t) + \frac{2L\kappa_n}{n\pi}\tanh\left(\frac{\pi n H}{2L}\right)\ddot{\alpha}(t)\right],$$

$$n = 1, 3, 5 \ldots \tag{4}$$

where $\omega_n = \sqrt{g\frac{\pi n}{L}\tanh\frac{\pi n H}{L}}$ indicates the natural sloshing frequencies. Once $\beta_n^P(t)$ have been found, $\Phi_P(x, z, t)$ can be calculated using the Equations (1), (2) and (3).

When the ship chamber is subjected to pure longitudinal motion, the sloshing can be described same as Faltinsen and Timokha [24]:

$$\frac{\partial^2\Phi_L}{\partial x^2} + \frac{\partial^2\Phi_L}{\partial z^2} = 0 \left(-\frac{L}{2} < x < \frac{L}{2}, -H < z < 0\right) \tag{5a}$$

$$\frac{\partial\Phi_L}{\partial x}\bigg|_{x=-\frac{L}{2},\frac{L}{2}} = \dot{x}(t) \tag{5b}$$

$$\frac{\partial\Phi_L}{\partial z}\bigg|_{z=-H} = 0 \tag{5c}$$

$$\left.\frac{\partial \Phi_L}{\partial z}\right|_{z=0} = \frac{\partial \eta_L}{\partial t} \tag{5d}$$

$$\left.\frac{\partial \Phi_L}{\partial t}\right|_{z=0} + g\eta_L = 0 \tag{5e}$$

$$\int_{-\frac{L}{2}}^{\frac{L}{2}} \eta_L dx = 0 \tag{5f}$$

here $\Phi_L(x, z, t)$ indicates the velocity potential under longitudinal motion, $\eta_L(x, t)$ denotes the free surface elevation under longitudinal motion. The exact procedures and solutions of Equations (5) are listed in Faltinsen and Timokha [24]:

$$\Phi_L(x, z, t) = \dot{x}(t)x + \sum_{n=1}^{\infty} \frac{\dot{\beta}_n^L(t)}{\kappa_n} \cos\left[\pi n \left(x + \frac{L}{2}\right)\bigg/ L\right] \frac{\cosh\left[\frac{\pi n(z+H)}{L}\right]}{\cosh\frac{\pi n H}{L}} \tag{6}$$

$$\ddot{\beta}_n^L(t) + \omega_n^2 \beta_n^L(t) = \ddot{x}(t)\frac{4}{n\pi}\tanh\left(\frac{n\pi H}{L}\right), \ n = 1, 3, 5\ldots \tag{7}$$

where $\beta_n^L(t)$ are the modal functions under pure longitudinal motion. Analogue to the linear superposition principle [28] used in Faltinsen and Timokha [24] to analyze 6DOF space motions, the $\beta_n(t)$ under coupled longitudinal and pitch motions can be expressed by linear superposition of $\beta_n^P(t)$ and $\beta_n^L(t)$:

$$\ddot{\beta}_n(t) + \omega_n^2 \beta_n(t) = \frac{4L}{\pi^2 n^2}\left[g\kappa_n\alpha(t) + \frac{2L\kappa_n}{n\pi}\tanh\left(\frac{\pi n H}{2L}\right)\ddot{\alpha}(t)\right.$$

$$\left. + \frac{n\pi}{L}\tanh\left(\frac{n\pi H}{L}\right)\ddot{x}(t)\right] \tag{8}$$

Then the absolute velocity potential $\Phi(x, z, t)$ under coupled longitudinal and pitch motions could be given by:

$$\Phi(x, z, t) = \dot{x}(t)x + \dot{\alpha}(t)\varphi_{sj}(x, z)$$

$$+ \sum_{n=1}^{\infty} \frac{\dot{\beta}_n(t)}{\kappa_n} \cos\left[\pi n \left(x + \frac{L}{2}\right)\bigg/ L\right] \frac{\cosh\left[\frac{\pi n(z+H)}{L}\right]}{\cosh\frac{\pi n H}{L}} \tag{9}$$

Based on the $\Phi(x, z, t)$, the total pressure p_T in the liquid can be expressed as:

$$p_T = p_0 - \rho g[z + x\alpha(t)] - \rho \frac{\partial \Phi}{\partial t} \qquad (10)$$

here p_0 is the pressure in the air, ρ is the water density, $-\rho g[z + x\alpha(t)]$ is the hydrostatic pressure. The last term $-\rho \frac{\partial \Phi}{\partial t}$ is the hydrodynamic pressure, which can be rewritten as:

$$p(x, z, t) = -\rho \ddot{x}(t)x - \rho \ddot{\alpha}(t)\varphi_{sj}(x, z)$$

$$- \rho \sum_{n=1}^{\infty} \frac{\ddot{\beta}_n(t)}{\kappa_n} \cos\left[\pi n \left(x + \frac{L}{2}\right) \bigg/ L\right] \frac{\cosh\left[\frac{\pi n(z+H)}{L}\right]}{\cosh \frac{\pi nH}{L}}$$

$$(11)$$

The total longitudinal hydrodynamic force F acting on the ship chamber walls, per unit width, is obtained from integration the hydrodynamic pressure over the wet areas, such that:

$$F = \int_{-H}^{0} [p(x, z, t)|_{x=\frac{L}{2}} - p(x, z, t)|_{x=-\frac{L}{2}}]dz \qquad (12)$$

While the hydrodynamic moment M about the point C, per unit width, can be determined by:

$$M = \int_{-H}^{0} [p(x, z, t)|_{x=\frac{L}{2}} - p(x, z, t)|_{x=-\frac{L}{2}}](z + H)dz$$

$$+ \int_{-\frac{L}{2}}^{\frac{L}{2}} p(x, z, t)|_{z=-H} x \, dx \qquad (13)$$

By properly integrating the pressure over the wet areas, the above moment and force can be expressed as:

$$F = -\rho LH \ddot{x}(t) - \frac{\rho LH^2}{2} \ddot{\alpha}(t) - \rho L^2 \sum_{n=1}^{\infty} \ddot{\beta}_n(t) \frac{[(-1)^n - 1]}{\pi^2 n^2} \qquad (14)$$

$$M_{CB} = -\frac{\rho L^3}{12} \ddot{x}(t) - \frac{\rho HL^3}{12} \ddot{\alpha}(t) + \rho L^3$$

$$\left\{ \ddot{\alpha}(t) \sum_{n=1}^{\infty} \frac{4L[(-1)^n - 1]^2}{\pi^5 n^5} \tanh\left(\frac{\pi nH}{2L}\right) - \sum_{n=1}^{\infty} \frac{\ddot{\beta}_n(t)}{\pi^3 n^3} \frac{[(-1)^n - 1]}{\sinh(\frac{\pi nH}{L})} \right\}$$

$$(15)$$

$$M_{CW} = -\frac{\rho L H^2}{2}\ddot{x}(t) - \frac{\rho L H^3}{6}\ddot{\alpha}(t)$$

$$- 4\rho L^3 \ddot{\alpha}(t) \sum_{n=1}^{\infty} \frac{[(-1)^n - 1]^2}{\pi^4 n^4} \left[\frac{2L}{\pi n}\tanh\left(\frac{n\pi H}{2L}\right)\right]$$

$$- \rho L \sum_{n=1}^{\infty} \frac{\ddot{\beta}_n(t)}{\pi n} \frac{[(-1)^n - 1]}{\sinh\left(\frac{\pi n H}{L}\right)}$$

$$\times \left[-\frac{L^2}{\pi^2 n^2}\left(\cosh\frac{\pi n H}{L} - 1\right) + \frac{HL}{\pi n}\sinh\left(\frac{\pi n H}{L}\right)\right] \qquad (16)$$

where M_{CB} denotes the hydrodynamic moment with respect to point C coming from the pressure on the bottom, M_{CW} denotes the hydrodynamic moment for point C resulting from the pressure on the wall.

2.2 Engineering Simplified Formulas

As shown in Table 1, the filling depth ratio for most of shiplifts currently being used in China are entirely less than 0.05. Base on the special situation, Equations (14), (15) and (16) would be further simplified for structural dynamics analysis and earthquake resistant design of the shiplift system.

As shown in Table 2, for the $H/L \leq 0.05$, M_{CB} has excellent convergence, only taking the lowest mode ($n = 1$) can control the error within 1.5%.

Table 1   Ratio of depth to length in different shiplifts

Shiplift Names	Current Status	Ratio of Depth to Length
Three Gorges shiplift	In use	0.0292
GouPitan shiplift/PengShui shiplift	In use	0.0424
GaoBazhou shiplift/GeHeyan shiplift	In use	0.0405
YanTan shiplift	In use	0.0468
TingZikou shiplift	In use	0.0216
ShuiKou shiplift	In use	0.0219

Table 2   Convergence of F, M_{CB}, and M_{CW} at different filling depth ratios under the condition of $x(t) = 0.11\sin\omega t$, $\alpha(t) = 0.0042\sin\omega t$, $\omega = 0.5$ Hz

	$F(\times 10^3\text{N})$			$M_{CB}(\times 10^5\text{N}\cdot\text{m})$			$M_{CW}(\times 10^3\text{N}\cdot\text{m})$		
H/L	$n=1$	$n=100$	$\frac{|\Delta F|}{F}$	$n=1$	$n=100$	$\frac{|\Delta M_{CB}|}{M_{CB}}$	$n=1$	$n=100$	$\frac{|\Delta M_{CW}|}{M_{Cw}}$
0.02	12.23	13.67	10.5%	57.02	57.72	1.21%	15.38	17.25	10.8%
0.03	19.00	21.18	10.3%	67.48	67.47	0.02%	33.53	38.49	12.9%
0.04	3.637	3.632	0.1%	3.410	3.401	0.26%	3.104	3.105	0.03%
0.05	4.365	4.288	1.8%	3.101	3.093	0.26%	3.712	3.711	0.03%

F and M_{CW} will generate an error of less than 11% and 13%, respectively. Moreover, it is evident that M_{CW} occupies less than 0.5% of the M_{CB}. That is, M_{CW} can be reasonably ignored in engineering design. It will be further validated in the following case simulations.

Through the above analysis, Equations (8), (14) and (15) can be further simplified by only retaining the lowest mode:

$$F_C = -\rho HL\ddot{x}(t) - \frac{\rho H^2 L}{2}\ddot{\alpha}(t) + \frac{2\rho L^2}{\pi^2}\ddot{\beta}_1(t) \quad (17)$$

$$M_C = -\frac{\rho L^3}{12}\ddot{x}(t) - \frac{\rho HL^3}{12}\ddot{\alpha}(t) + \frac{8\rho HL^3}{\pi^4}\ddot{\alpha}(t)$$

$$+ \frac{2\rho L^4}{\pi^4 H}\ddot{\beta}_1(t) \quad (18)$$

$$\ddot{\beta}_1(t) + \omega_1^2\beta_1(t) = \frac{4Hg}{L}\alpha(t) + \frac{4H^2}{L}\ddot{\alpha}(t) + \frac{4H}{L}\ddot{x}(t) \quad (19)$$

here F_C is the longitudinal hydrodynamic force, M_C is the total hydrodynamic moment, $\beta_1(t)$ is the lowest modal function and ω_1 is the lowest natural frequency of the contained fluid. Equations (17) to (19) are more applicable to the calculation of hydrodynamic pressure and force when the ship chamber encounters longitudinal and pitch coupling motion under non-seismic conditions. And the liquid filling ratio of the ship chamber must be less than 0.05 ($H/L < 0.05$).

3 Results and Discussion

To validate and analyze the reliability of the above formulas, two main test cases have been conducted. For both cases, a two-dimensional ship chamber (part of the Three Gorges shiplift) is used. The filling depth ratio is 0.03, with $H = 3.5$ m and $L = 120$ m. The first case is to compare the free surface elevation under coupled motions. While the second one is to compare the longitudinal force and hydrodynamic moment under earthquake and non-earthquake conditions.

3.1 Validation

Sloshing caused by the coupled motions would be validated by comparing the free surface elevation. Based on the linear shallow water theory [16], η_s

under coupled motions can be derived as:

$$\eta_s = -\ddot{x}(t)\frac{L\omega_1}{\pi\omega}\frac{1/g}{\cos(\pi\omega/2\omega_1)}\sin\frac{\pi\omega x}{L\omega_1}$$

$$+ \alpha(t)\left[x - \frac{L\omega_1}{\pi\omega}\frac{1+3.5\omega^2/g}{\cos(\pi\omega/2\omega_1)}\sin\frac{\pi\omega x}{L\omega_1}\right] \tag{20}$$

where η_s is the free surface elevation obtained by linear shallow water theory, $x(t) = x_{max}\sin\omega t$ indicates the longitudinal motion, $\alpha(t) = \alpha_{max}\sin\omega t$ represents the pitch motion.

While the the free surface elevation $\eta(x,t)$ under coupled longitudinal and pitch motions derived by linear modal theory could be given by:

$$\eta(x,t) = \sum_{n=1}^{\infty}\beta_n(t)\cos\left[\pi n\left(x + \frac{L}{2}\right)\middle/L\right] \tag{21}$$

According to the constraints of the actual engineering conditions of the Three Gorges shiplift, $x_{max} = 0.11$ m, $\alpha_{max} = 0.0042$ rad and $\omega/\omega_1 = 0.6$ are set. The η_s (triangle symbol) and η (round symbol) are then observed in Figure 2.
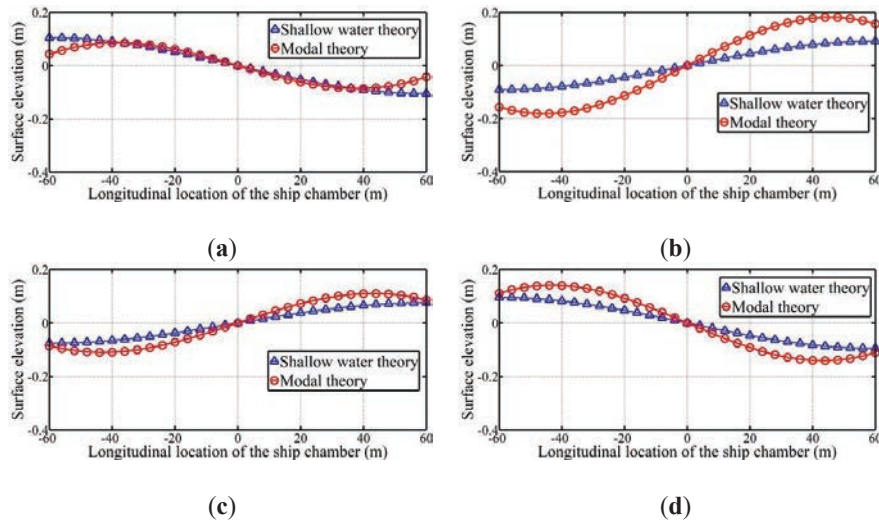

Figure 2 Comparison of the free surface elevation between η_s (triangle symbol) and η (round symbol) at $t = 20$ s (a), $t = 45$ s (b), $t = 60$ s (c) and $t = 80$ s (d) under coupled motions, $x(t) = 0.11\ sin\omega t$, $\alpha(t) = 0.0042\ sin\omega t$, $\omega/\omega_1 = 0.6$.

η_s and η are compared at four different times ($t = 20$ s, 45 s, 60 s, 80 s), which are any four times in a cycle. It is obvious that η derived by linear modal theory provides a good match with the linear shallow water theory. The maximum difference at the ship chamber walls ($x = \pm 60$ m) is 0.0659 m ($t = 20$ s), which is much smaller than the water depth, $H = 3.5$ m. The occurrence of such a phenomenon well explained that it is suitable to apply the linear modal theory to simulate the shallow water sloshing in the ship chamber under coupled motions.

3.2 Hydrodynamic Moment

A further comparison between the Housner model (currently widely used in the shiplift seismic design) and the Equations (17) to (19) is shown in Tables 3 and 4.

As shown in Table 3, M_C, M_L and M_P are the hydrodynamic moments under coupled motions, pure longitudinal motion and pure pitch motion, respectively. While M_{HM} is the hydrodynamic moment directly calculated by the Housner model. M_{HM} only has a small growth with 2x increase in peak acceleration under earthquake condition. More than this, there is little difference for M_{HM} under seismic or non-seismic condition. Such behavior is rather unreasonable in comparison to M_C, which has an obvious grow up with the rise of earthquake intensity. In addition, M_C under non-seismic condition is much smaller than seismic condition. Incidentally, this confirms the correctness of Equation (18).

Table 3   Hydrodynamic moment under different working conditions, $\ddot{x}(t) = 0.1gsin\omega t/$ $0.2gsin\omega t/0.4gsin\omega t/ - \omega^2 0.11sin\omega t$, $\alpha(t) = 0.0042sin\omega t$, $\omega/\omega_1 = 0.7$

Earthquake Intensity	$M_C(\text{N} \cdot \text{m})$	$M_L(\text{N} \cdot \text{m})$	M_P/M_C	$M_{HM}(\text{N} \cdot \text{m})$
7	4.596×10^8	4.466×10^8	2.83%	5.241×10^6
8	9.062×10^8	8.931×10^8	1.45%	5.955×10^6
9	1.799×10^9	1.786×10^9	0.72%	7.383×10^6
Non-earthquake	4.799×10^7	3.488×10^7	27.32%	4.526×10^6

Table 4   Longitudinal force under different working conditions, $\ddot{x}(t) = 0.1gsin\omega t/0.2gsin$ $\omega t/0.4gsin\omega t/ - \omega^2 0.11sin\omega t$, $\alpha(t) = 0.0042sin\omega t$, $\omega/\omega_1 = 0.7$

Earthquake Intensity	$F_C(\text{N})$	$F_L(\text{N})$	F_P/F_C	$F_{HM}(\text{N})$
7	1.174×10^6	1.143×10^6	2.64%	1.242×10^4
8	2.317×10^6	2.285×10^6	1.38%	1.935×10^4
9	4.602×10^6	4.571×10^6	0.67%	3.321×10^4
Non-earthquake	1.152×10^5	8.370×10^4	27.34%	5.476×10^3

Since M_C is composed by two parts (M_L and M_P), it allows to investigate the respective degree of contribution. For the earthquake resistant design, M_P could be neglected (the largest proportion is less than 3%) to further simplify Equation (18). However, M_P should be reserved (accounting for up to 27.32%) under the non-earthquake condition. This meaning that while the ship chamber is subjected to longitudinal seismic, Equations (18) and (19) can be further simplified as:

$$M_C = -\frac{\rho L^3}{12}\ddot{x}(t) + \frac{2\rho L^4}{\pi^4 H}\ddot{\beta}_1(t) \tag{22}$$

$$\ddot{\beta}_1(t) + \omega_1^2\beta_1(t) = \ddot{x}(t)\frac{4}{\pi}\tanh\frac{\pi H}{L} \tag{23}$$

Analysis results display that the Equations (22) and (23) are more applicable to the calculation of hydrodynamic pressure when the ship chamber encounters longitudinal earthquake. Meanwhile, the liquid filling ratio of the ship chamber must be less than 0.05 ($H/L < 0.05$).

It can be seen from the Figure 3 that whether seismic or non seismic conditions, the hydrodynamic moment changes periodically and does not diverge. This is because the influence of water sloshing damping is not considered in the calculation process. Figure 3 shows that the hydrodynamic moment tends to converge under both seismic and non seismic conditions, that is, the motion of the ship chamber tends to converge.

3.3 Hydrodynamic Force

The longitudinal force resulting from the sloshing plays a crucial role in the design of longitudinal guiding mechanism. Table 4 displays the variation of
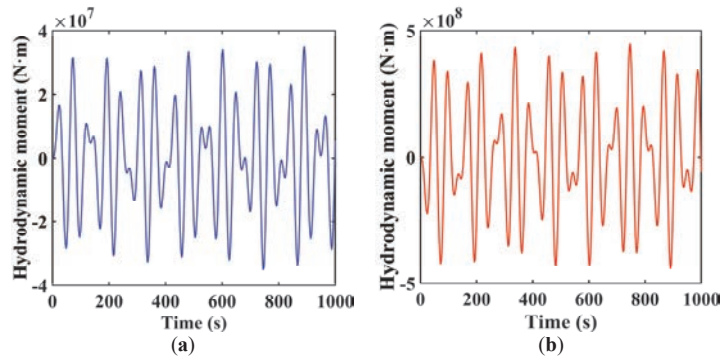

Figure 3   The hydrodynamic moment change with time under the condition of non earthquake (a) and earthquake with magnitude 7 (b) in Table 3.

longitudinal force under different conditions. F_C, F_L and F_P are the forces under coupled motions, pure longitudinal motion and pure pitch motion, respectively. F_{HM} stands for the hydrodynamic force calculated by the Housner model.

Similarly to the previous case, both F_{HM} and F_L are the forces under pure longitudinal motion. It is worth noting that F_{HM} is far less than F_L derived by Equation (17). Meanwhile, F_L has an obvious growth with 2x increase in peak acceleration under earthquake condition. The difference between the seismic and non-seismic condition is more evident. That is, F_L is more suitable to calculate the hydrodynamic force in the ship chamber. Apart from this, Table 4 also points out that F_P accounts for less than 3% of F_C under earthquake condition. Nevertheless, the proportion reaches 27.34% in non-seismic condition. This means that Equation (17) is in agreement with the non-seismic condition. But for seismic condition, Equation (17) can be further simplified as:

$$F_C = -\rho L H \ddot{x}(t) + \frac{2\rho L^2}{\pi^2} \ddot{\beta}_1(t) \tag{24}$$

The analysis results show that the Equation (24) is more suitable for the calculation of hydrodynamic force when the ship chamber encounters longitudinal earthquake. The liquid filling ratio of the ship chamber must be less than 0.05 ($H/L < 0.05$) simultaneously.

It can be seen from the Figure 4 that the hydrodynamic force shows periodic oscillation changes in 0 to 1000 seconds. If the damping of water sloshing is taken into account, the peak value of the curve will eventually gradually attenuate and tend to converge. That is to say, the motion of the ship chamber will eventually show convergence.
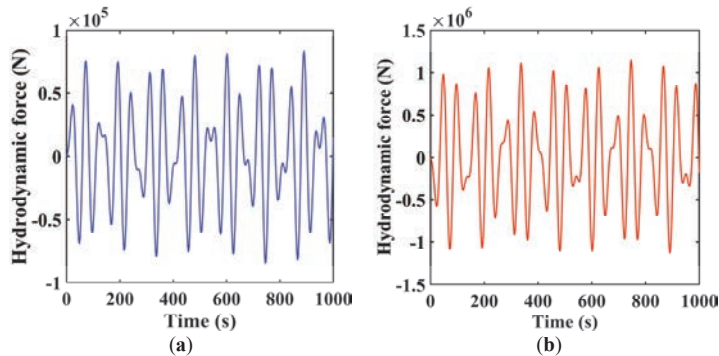

Figure 4 The hydrodynamic force change with time under the condition of non earthquake (a) and earthquake with magnitude 7 (b) in Table 4.

4 Conclusions

An analytical methodology founded on the linear modal theory is newly presented to investigate the shallow water sloshing in the ship chamber under coupled longitudinal and pitch motions resulted by longitudinal earthquake. Engineering simplified formulations of the hydrodynamic moment and force are derived by using the linear superposition principle. The applicability of the proposed method is demonstrated against comparing with the linear shallow water theory of Verhagen and Wijngaarden [16]. Case simulations under seismic and non-seismic conditions illustrate the accuracy of proposed formulas with respect to the Housner model. The key observations are summarized as follows.

(1) For the ship chamber, a modal system describing the shallow water sloshing is developed. Within the allowable range of shiplift engineering precision, the infinite set of modal functions ($n = 1, 3, 5\ldots$) could be accurately reduced with only retaining the lowest mode ($n = 1$). The maximum error of hydrodynamic moment and force between $n = 1$ and $n = 100$ are lower than 1.3% and 10.5%, respectively. The convergence error comparing with the currently widely used Housner model (hydrodynamic moment 1.5% and hydrodynamic force 55%) is greatly improved.

(2) For the rectangular ship chamber with filling depth ratio less than 0.05, the hydrodynamic moment resulting from pressure on the walls can be reasonably ignored regardless of earthquake, which accounts for less than 0.5% percent of total hydrodynamic moment.

(3) The newly proposed engineering formulas of hydrodynamic moment and force can be used to simulate the shallow water sloshing in ship chamber and rectangular liquid storage container with similar filling ratio. In addition, it can effectively supplement the missing part of longitudinal seismic calculation part in the current design code for shiplift.

Funding Statement

Data Availability

The data used to support the findings of this study are included within the article.

Conflicts of Interest

The authors declare that there is no conflict of interest regarding the publication of this paper.

References

[1] Housner, G. W. Earthquake pressures on fluid containers. Report EERL-1954-3, Earthquake Engineering Research Laboratory, California Institute of Technology, Pasadena, 1954.

[2] Housner, G. W. Dynamic pressures on accelerated fluid containers. B. Seismol. Soc. Am. 47(1) (1957) 15–35.

[3] Housner, G. W. The dynamic behavior of water tanks. B. Seismol. Soc. Am. 53(2) (1963) 381–387.

[4] Cheng, X., Shi, D., Li, H., Xia, R., Zhang, Y., Zhou, J. Stability and parameters influence study of fully balanced hoist vertical ship lift. Struct. Eng. Mech. 66(5) (2018) 583–594. doi: 10.12989/sem.2018. 66.5.583.

[5] Zhang, Y., Shi, D., Shi, L., Xia, R., Cheng, X., Zhou, J. Analytical solution of capsizing moments in ship chamber under pitching excitation. P. I. Mech. Eng. C-J. Mec, 2019. https://doi.org/10.1177/095440621984 3327.

[6] Chen, B. F. Viscous fluid in tank under coupled surge, heave, and pitch motions. J. Waterw. Port. Coast. 131(5) (2005) 239–256. DOI: 10.1061/ (ASCE)0733-950X(2005)131:5(239).

[7] Stephen, J. J., Sannasiraj, S. A., Sundar, V. Numerical simulation of sloshing in a rectangular tank under combined horizontal, vertical and rotational oscillations. P. I. Mech. Eng. M-J. Eng. 230(1) (2016) 95–113. DOI: 10.1177/1475090214533512.

[8] Graham, E. W., Rodriguez, A. M. Characteristics of fuel motion which affect airplane dynamics. J. Appl. Mech-T. ASME. 19 (1952) 381–388.

[9] Eide, D. G. Preliminary analysis of variation of pitch motion of a vehicle in a space environment due to fuel sloshing in a rectangular tank, NASA TN-D-2336, 1964.

[10] Abramson, H. N. The dynamic behavior of liquids in moving containers. NASA Special Publication 106(7) (1966).

[11] Dodge FT. The new dynamic behavior of liquids in moving containers. [Update of NASA SP-106]. San Antonio, Texas: Southwest Research Institute, 2000.

[12] Ibrahim, R. A. Liquid Sloshing Dynamics: Theory and Applications. Cambridge University Press, Cambridge, 2005. DOI: 10.1017/CBO978 0511536656.015.

[13] Liao, L.K. Safety analysis and design of full balanced hoist vertical shiplifts. Struct. Eng. Mech. 49(3) (2014) 517–522. DOI: 10.12989/s em.2014.49.3.311.

[14] Li, Y., Di, Q., Gong, Y. Equivalent mechanical models of sloshing fluid in arbitrary section aqueducts. Earthquake. Eng. Struct. Dyn. 41(6) (2012) 1069–1087. DOI: 10.1002/eqe.1173.

[15] Li, Y., Wang, J. A supplementary, exact solution of an equivalent mechanical model for a sloshing fluid in a rectangular tank. J. Fluid. Struct. 31(5) (2012) 147–151. DOI: 10.1016/j.jfluidstructs.2012.02.012.

[16] Verhagen, J. H. G., Wijngaarden, L. V. Non-linear oscillations of fluid in a container. J. Fluid. Mech. 22(4) (1965) 737–751. DOI: 10.1017/S0 022112065001118.

[17] Antuono, M., Bouscasse, B., Colagrossi, A., Lugni, C. Two-dimensional modal method for shallow-water sloshing in rectangular basins. J. Fluid. Mech. 700(6) (2012) 419–440. DOI: 10.1017/jfm.2012.140.

[18] Antuono, M., Brocchini, M. Beyond boussinesq-type equations: semi-integrated models for coastal dynamics. Phys. Fluids. 25(1) (2013) 815–827. DOI: 10.1063/1.4774343.

[19] Antuono, M., Bardazzi, A., Lugni, C., Brocchini, M. A shallow-water sloshing model for wave breaking in rectangular tanks. J. Fluid. Mech. 746(3) (2014) 437–465. DOI: 10.1017/jfm.2014.127.

[20] Antuono, M., Lugni, C. Global force and moment in rectangular tanks through a modal method for wave sloshing. J. Fluid. Struct. 77 (2018) 1–18. DOI: 10.1016/j.jfluidstructs.2017.11.004.

[21] Faltinsen, O.M., Rognebakke, O.F., Lukovsky, I.A., and Timokha, A.N. Multidimensional modal analysis of nonlinear sloshing in a rectangular tank with finite water depth. J. Fluid. Mech. 407 (2000) 201–234. DOI: 10.1017/S0022112099007569.

[22] Faltinsen, O.M., and Timokha, A.N. An adaptive multimodal approach to nonlinear sloshing in a rectangular tank. J. Fluid. Mech. 432 (2001) 167–200. DOI: 10.1088/1468-5248/2/1/007.

[23] Faltinsen, O.M., and Timokha, A.N. Asymptotic modal approximation of nonlinear resonant sloshing in a rectangular tank with small fluid depth. J. Fluid. Mech. 470 (2002) 319–357. DOI: 10.1017/S0022112 002002112.

[24] Faltinsen, O.M., and Timokha, A.N. Sloshing. Cambridge University Press, 2009.

[25] Strand, I. M., Faltinsen, O.M. Linear sloshing in a 2D rectangular tank with a flexible sidewall. J. Fluid. Struct. 73 (2017) 70–81. https://doi.org/10.1016/j.jfluidstructs.2017.06.005.

[26] Kolaei, A., Rakheja, S., Richard, M. J. Coupled multimodal fluid-vehicle model for analysis of anti-slosh effectiveness of longitudinal baffles in a partially-filled tank vehicle. J. Fluid. Struct. 70 (2017) 519–536. DOI: 10.1016/j.jfluidstructs.2017.02.012.

[27] Zhang Y, Shi D, Liao L, et al. Pitch stability analysis of high-lift wire rope hoist vertical shiplift under shallow water sloshing-structure interaction. Proceedings of the Institution of Mechanical Engineers. Part K, Journal of Multi-body Dynamics. 233(4) (2019) 942–955. DOI: 10.1177/1464419319850666.

[28] Haberman, Richard. Applied partial differential equations: with Fourier series and boundary value problems: International Edition. Pearson Schweiz Ag, 2012.

Biographies

Jianbao Yang, a lecturer at Hubei University of Science and Technology, he earned a Master's degree from Shihezi University, Xinjiang, China, in 2017. His current research interests include fluid mechanics, medical engineering, neural network.

Yang Zhang, a lecturer at Hubei University of Science and Technology, he earned a Doctor of Engineering from Wuhan University, Wuhan, China, in 2020. His current research interests include shiplift, fluid mechanics, fluid-structure coupling, multi-body dynamics.

Duanwei Shi, professor and doctoral advisor of Wuhan University. Research direction: mechanical system dynamics, virtual prototyping technology, CAE. The research on the dynamic performance of the main structures of the three gorges shiplift, Xiangjiaba shiplift, Danjiangkou shiplift, Pengshui shiplift and Gaobazhou shiplift has been completed.